

# Iterative correction process for optical thin film synthesis with the Fourier transform method

P. G. Verly and J. A. Dobrowolski

Several errors inherent to the Fourier transform method for optical thin film synthesis, including the inaccuracy of the spectral functions  $\tilde{Q}(\sigma)$  used in the Fourier transforms, are compensated numerically by using successive approximations. We show that the complex phase of  $\tilde{Q}(\sigma)$  is a key parameter which can be exploited to reduce significantly the thickness of the synthesized films and to control the shape of the refractive index profiles without affecting the spectral performance. This method is compared to other well established thin film design techniques.

## I. Introduction

Graded index films<sup>1-5</sup> have a number of potential advantages over the more classical coatings composed of homogeneous multilayers. As yet they are difficult to produce, but efforts to implement this technology are under way in several laboratories. Important practical applications include rugate filters, wideband antireflection coatings, and nonpolarizing beam splitters.

The Fourier transform method<sup>6-10</sup> is one of the few approaches available for the synthesis of such films. It is fast and very versatile, and it can also yield homogeneous multilayers. Essentially, it is based on a Fourier transform relationship between the logarithmic derivative  $1/n \, dn/dx$  of the refractive index profile and a complex spectral function  $\tilde{Q}(\sigma)$  which depends on the desired spectral performance.

A proper definition of  $\tilde{Q}(\sigma)$  is essential for accuracy. The analytical forms of  $\tilde{Q}(\sigma)$  known so far are only approximate, especially for problems in which there is a high reflectance.<sup>6-12</sup> This can be compensated to some extent by empirical adjustments when the spectral shapes are simple.<sup>10</sup> Better forms of  $\tilde{Q}(\sigma)$  are needed for more general applications. Sossi<sup>6,7</sup> proposed overcoming this limitation numerically by successive approximations. His iterative correction process also compensates simultaneously for several other errors inherent to the Fourier transform method. Unfortunately, it has only been tested with a few simple examples.

In this paper, we describe a modified version of Sossi's correction process. We discuss the influence of several key parameters not addressed before and in particular the complex phase of  $\tilde{Q}(\sigma)$ . In our procedure, this phase is exploited to reduce significantly the optical thickness of the synthesized films and to control the shape of the refractive index variations without affecting the spectral performance. We show by a number of numerical examples that good results are possible.

In Sec. II, we briefly review the basic Fourier transform method and Sossi's correction process. In Sec. III, we describe the modifications implemented in our version and the flow of the calculations in our computer program. Sections IV and V are devoted to numerical examples. The effects of several optional parameters are illustrated, and some limitations are pointed out. The performance of the process is compared with that of other well established techniques. A design obtained by the present method for an arbitrary problem is compared to published solutions. Finally, a discussion is included in Sec. VI.

## II. Background

### A. Basic Fourier Transform Method

The Fourier transform method described here is based on Sossi's original work.<sup>6,7,9</sup> The notation is essentially the same as that used in a previous paper.<sup>10</sup> As before, we consider a gradual refractive index profile  $n(x)$  sandwiched between identical media without refractive index steps. If the usual assumptions are made (normal incidence, no dispersion, no absorption), a simple relationship

$$n(x) = n_0 \exp \left[ \frac{j}{\pi} \int_{-\infty}^{\infty} \frac{\tilde{Q}(\sigma)}{\sigma} \exp(-j2\pi\sigma x) d\sigma \right] \quad (1)$$

exists between  $n(x)$  and a complex spectral function

The authors are with National Research Council of Canada, Physics Division, Ottawa, Ontario K1A 0R6, Canada.

Received 22 November 1989.

0003-6935/90/253672-13\$02.00/0.

© 1990 Optical Society of America.

$$\tilde{Q}(\sigma) = Q[T(\sigma)] \exp[j\phi(\sigma)], \quad (2)$$

which depends on the desired transmittance  $T(\sigma)$ . In the above equations,  $\sigma$  is the wavenumber  $1/\lambda$ , where  $\lambda$  is the wavelength,  $n_0$  is the refractive index of the surrounding media,  $x$  is twice the optical thickness,

$$x = 2 \int_0^z n(u) du, \quad (3)$$

and  $z$  is the metric thickness. The quantity between the brackets in Eq. (1) is a Fourier transform. {Thus the logarithm  $\ln[n(x)]$  and  $\tilde{Q}(\sigma)/\sigma$  constitute a Fourier transform pair within a (complex imaginary) multiplicative constant; the logarithmic derivative  $1/n \, dn/dx$  and  $\tilde{Q}(\sigma)$  constitute another pair.} Since  $n(x)$  must be real, the complex function  $\tilde{Q}(\sigma)$  is defined for negative wavenumbers by the symmetries  $\tilde{Q}(-\sigma) = \tilde{Q}^*(\sigma)$ , where the superscript \* denotes a complex conjugate. In the following,  $\tilde{Q}(\sigma)$  and its complex phase  $\phi(\sigma)$  will be referred to as the  $Q$ -function and the  $Q$ -phase, respectively.

Equation (1) forms the basis of this thin film synthesis method. It relates the unknown refractive index profile  $n(x)$  to the desired spectral characteristics via the  $Q$ -function. Several approximate analytical forms of the latter have been reported. They are valid in principle only for low reflectances. To a first approximation, it can be shown that<sup>7,8</sup>

$$\tilde{Q}(\sigma) = \frac{r(\sigma)}{t(\sigma)}. \quad (4)$$

The parameters  $r$  and  $t$  are, respectively, the complex reflection and transmission coefficients for the amplitude of the electromagnetic field. The phase of  $r/t$  is the  $Q$ -phase. Equation (4) means that the  $Q$ -phase is approximately equal to the phase  $\arg(r/t)$  of a film which is a good solution of the synthesis problem. The  $Q$ -phase to be used initially in the synthesis is usually unknown because the phase on reflection or transmission is rarely specified, and especially not the phase of  $r/t$ . Many different films, corresponding to different phases, can be obtained for a prescribed reflectance ( $R = |r|^2$ ) or transmittance ( $T = |t|^2$ ).

Equation (4) requires that the origin of the thickness coordinate  $x$  and  $z$  be in the center of the film. Otherwise the right-hand side of Eq. (4) has to be multiplied by a phase factor which takes into account the position of the origin. Throughout this paper the thicknesses will be measured from the center out.

Several other forms of  $\tilde{Q}$  have also been proposed.<sup>6,9-12</sup> Only the magnitude  $Q[T(\sigma)]$  of  $\tilde{Q}(\sigma)$  is calculated, and the  $Q$ -phase is arbitrary. For example,

$$Q_2(T) = \sqrt{1 - T}, \quad (5a)$$

$$Q_3(T) = \sqrt{\frac{R}{T}} = \sqrt{\frac{1}{T} - 1}, \quad (5b)$$

$$Q_4(T, w) = wQ_2(T) + (1 - w)Q_3(T), \quad (5c)$$

$$Q_5(T) = \ln(\gamma + \sqrt{\gamma^2 - 1}), \quad (5d)$$

where

$$\gamma = 1 + \frac{1}{4} \left( \frac{1}{T} - T \right). \quad (5e)$$

The subscripts of the  $Q$  terms in the above equations correspond to the notation used in Ref. 10, and  $w$  is an arbitrary constant which can be adjusted to improve the spectral fit. Some of the above functions have been plotted against transmittance in Fig. 1. The curves diverge for low transmittances, because, as mentioned, the theory is an approximation in this region.

The  $Q$ -functions are most commonly used in the form described in Eq. (5). The simplest alternative for the selection of the arbitrary  $Q$ -phase  $\phi(\sigma)$  is to keep it constant. However, a proper choice of  $\phi(\sigma)$  can improve the spectral fit and/or control the distribution of the refractive index changes.<sup>9,10</sup>

## B. Sossi's Correction Method

For elementary spectral shapes, several key parameters used in the synthesis can be optimized manually. Good results can be obtained even when the reflectance is high.<sup>10</sup> This is difficult for more general applications and will remain so until better analytical expressions for the  $Q$ -function are found. Alternatively, Sossi showed that a good solution can be obtained numerically by successive approximations. He proposed two versions of a process based essentially on the following principle.

In the first implementation,<sup>6</sup> the  $Q$ -function remains real [ $\phi(\sigma) = 0$ ]. A film synthesized by using Eqs. (1)–(5) directly has a transmittance  $T$  which is usually different from the desired transmittance  $T_D$ . As a result, the values of  $Q(T)$  obtained by substituting back  $T$  into the  $Q$ -function are different from those of  $Q(T_D)$ , which were used initially in the Fourier transform to compute the refractive index profile. Sossi suggested that, by adding the difference of these two quantities to the old values of the  $Q$ -function, an improved  $Q$ -function might be obtained:

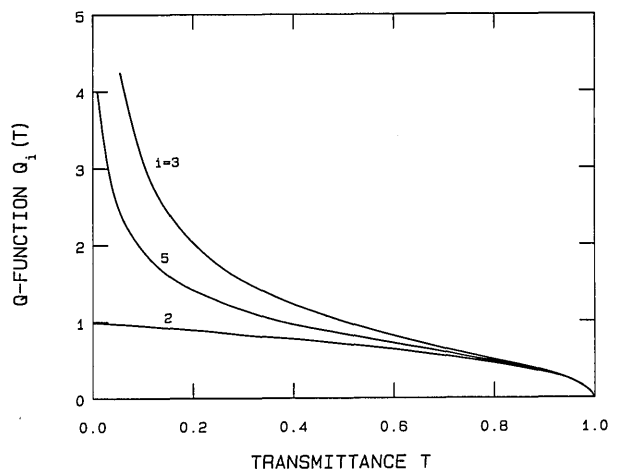


Fig. 1. Variation of several  $Q$ -functions  $Q_i(T)$  against transmittance.  $Q_4(T, w)$  is represented by a family of intermediate curves depending on the value of  $w$ . For example,  $Q_4(T, 1) \equiv Q_2(T)$ ,  $Q_4(T, 0.85) \approx Q_5(T)$ ,  $Q_4(T, 0) \equiv Q_3(T)$ .

$$Q_{i+1}(\sigma) = Q_i(\sigma) + \Delta Q_i(\sigma) \quad i = 1, 2, 3, \dots, \quad (6a)$$

$$\Delta Q_i(\sigma) = Q[T_D(\sigma)] - Q[T_i(\sigma)], \quad (6b)$$

$$Q_1(\sigma) = Q[T_D(\sigma)]. \quad (6c)$$

The subscripts  $i$  in Eq. (6) refer to successive iterations since, of course, the operation can be repeated several times.

In the second version,<sup>7</sup> the method is generalized for the case of a complex  $Q$ -function [namely,  $\bar{Q}(\sigma) = r/t$ ]. Here the  $Q$ -phase  $\phi(\sigma)$  is the physical phase  $\arg(r/t)$ , but the phases of  $r$  and  $t$  are not specified. The desired spectral quantity is again  $T_D$ . A target phase is fixed arbitrarily at the outset, and the real and imaginary parts of the  $Q$ -function ( $Q \cos \phi$  and  $Q \sin \phi$ ) are adjusted by iterations with equations similar to Eqs. (6).

The refractive index profiles found from Eqs. (1) and (6) often need to be modified in practice. For example, the gradual refractive index variations might be approximated by a homogeneous multilayer system (discretization), or they might be forced to lie within specified upper and lower limits ( $n_H, n_L$ ) or they might be neglected beyond a certain overall maximum thickness (truncation). These additional approximations result in a further deterioration of the spectral performance. A partial compensation is possible because  $T_i$  in Eq. (6) is the transmittance of the final refractive index profile obtained after the modifications.

This method has an interesting potential, but further testing is required because Sossi illustrated his theory with only a few simple examples. Several important practical points discussed in the following sections were also not addressed.

### III. Modified Correction Method

Instead of working with real and imaginary parts of the complex  $Q$ -functions, we prefer to focus on their magnitude and phase. One reason is that the error in  $Q$  is closely related to that in  $T$ , the quantity of interest, and it is easily calculated. Another is that the  $Q$ -phase is a free parameter which should be allowed to change if, by doing so, the results can be improved. It will be shown that the overall thickness required for a solution can be reduced significantly when the spectral variation of the  $Q$ -phase is chosen appropriately. This is an important practical consideration which we believe has not been discussed before.

In this work the correction applied to the  $Q$ -function is given by a modified form of Eq. (6):

$$\bar{Q}_{i+1}(\sigma) = \bar{Q}_i(\sigma) + s_i \Delta \bar{Q}_i(\sigma) \quad i = 1, 2, 3, \dots, \quad (7a)$$

$$\Delta \bar{Q}_i(\sigma) = \Delta Q_i(\sigma) \exp[j\psi_i(\sigma)], \quad (7b)$$

$$\Delta Q_i(\sigma) = Q[T_D(\sigma)] - Q[T_i(\sigma)], \quad (7c)$$

$$Q_1(\sigma) = Q[T_D(\sigma)] \exp[j\phi_1(\sigma)]. \quad (7d)$$

Three new key parameters have been introduced— $s_i$ ,  $\psi_i(\sigma)$ , and  $\phi_i(\sigma)$ . The step size  $s_i$  is a variable which can be adjusted to control the magnitude of the correction performed in each iteration. The complex phase  $\psi_i(\sigma)$  is used to ensure that the corrections add up

constructively. The initial  $Q$ -phase  $\phi_1(\sigma)$  controls the synthesis of the starting design which will be modified by the correction process.

The term correction process in this paper refers to the procedure by which the corrected  $Q$ -functions ( $\bar{Q} + s\Delta\bar{Q}$ ) and improved refractive index profiles are found. In particular, the process involves the computation of the optimum parameters  $s_i$  and  $\psi_i(\sigma)$ . The spectral shape of  $\phi_1(\sigma)$  is determined separately at the outset of the synthesis.

### B. Block Diagram

Our version of the correction process and the procedure to determine the initial  $Q$ -phase  $\phi_1(\sigma)$  have been added to the previously described NRCC software for synthesis with the Fourier transform method.<sup>9</sup> Figure 2 summarizes graphically the flow of the calculations which pertains to the correction process. Only the main options are indicated. Details can be found in the text below.

Required input data for the main program (Fig. 2, A) are the target transmittance, the optical thickness beyond which the film must be truncated, the desired form of the  $Q$ -function, and the initial spectral shape of the  $Q$ -phase  $\phi_1(\sigma)$ . Any analytical form of  $Q$  can be used including those listed in Eqs. (5). The phase  $\phi_1(\sigma)$  can be optimized either manually without leaving the program (B) or by refinement (C). A graded index film is then synthesized (D) with this complex  $Q$ -function (magnitude and phase). If desired, it can be transformed subsequently into a homogeneous multilayer, and/or the refractive indices can be forced to lie between prescribed values  $n_H, n_L$ . This can be done

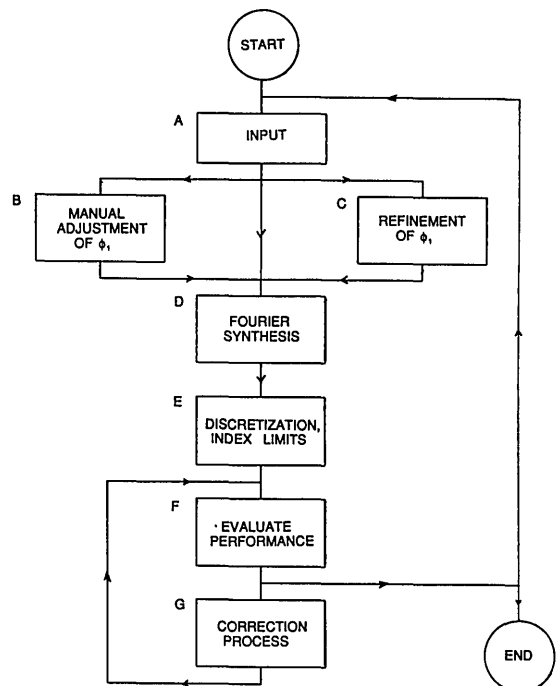


Fig. 2. Flow of the calculations pertaining to the correction process.

interactively or automatically (*E*). The design and its spectral performance are plotted on a graphic output (*F*). Several options are then selected at will: (1) the program can be stopped if the solution is satisfactory; (2) the synthesis can be repeated with new input parameters; or (3) the correction process can be invoked (*G*). Two versions of the latter are available. They differ in the method used to optimize the magnitude of the corrections. One version is faster, whereas the other is useful when nonuniform tolerances are specified for the transmittances. As in the main program, the corrected refractive index profiles can be graded or discretized, or they can be clipped to lie within a specified range of refractive index values.

The correction process is controlled by several optional input parameters which can be entered interactively. They include the *Q*-function (which can be different from the one used in the main program), the tolerances, the minimum acceptable rate of convergence, the initial step size, and the maximum number of iterations. Default values are also available. The process can be interrupted at any time without aborting the program and modified with new input parameters. Several different *Q*-functions and/or tolerances can be used successively. It is also possible to change the number of points at which the profile is calculated, the number of spectral points and the spectral range (for example, it might be extended to obtain a better fit at the ends of the desired range). Finally a whole new synthesis can also be attempted, for example, with a new *Q*-phase found from the results of the previous synthesis.

## B. Magnitude of the Corrections

As mentioned previously, our correction process is based on the calculation and examination of the refractive index profiles resulting from Eqs. (1) and (7a)–(7d). This section and the next are concerned with a more detailed discussion of the magnitude ( $s \cdot \Delta Q$ ) and phase  $\psi$  of the corrections made to the *Q*-functions.

Paramount in our correction subroutine is the optimization of the step size *s* to maintain a satisfactory convergence rate in the computations. This is done by calculating a scalar merit function<sup>13</sup>

$$M = \left\{ \frac{1}{N} \sum_{i=1}^N \left[ \frac{T(\sigma_i) - T_D(\sigma_i)}{\delta T(\sigma_i)} \right]^2 \right\}^{1/2}, \quad (8)$$

which characterizes the spectral performance of the resulting refractive index profile (multilayer or graded index film). Here the  $\sigma$  terms are the wavenumbers used in the computations (normally interpolated at equal wavenumber increments from the points at which the target curve is initially specified), and the  $\delta T$  terms are acceptable transmittance tolerances.

Two options are available to determine *s*. One possibility is to increment *s* in each iteration until the value of *M* reaches a minimum. Alternatively, *s* may be changed only if *M* does not converge properly: should *M* increase, *s* is divided by two and the iteration is repeated; should *M* decrease too slowly, *s* is doubled for the next iteration. The process is stopped when no

further improvement can be made or when a predetermined maximum number of iterations has been reached.

Each option for the selection of *s* has its advantages and disadvantages. When *s* is fully optimized in each iteration, the correction process is more sensitive to the actual values of *M* and, in particular, to the prescribed tolerances. This is useful when nonuniform tolerances are utilized to force the spectral fit in a particular wavelength region. The other option is often faster because fewer tentative steps are wasted, and, therefore, fewer computations of the performance of the system are required. Normally we use the latter option—exceptions will be mentioned in the numerical examples. Both options yield essentially the same films when the tolerances are uniform.

The successive corrections  $\Delta \bar{Q}$  result in new refractive index profiles. Although the latter could be obtained from Eqs. (1) and (7), we find it expedient to use the following explicit expressions:

$$n_{i+1}(x) = n_i(x) \Delta n_i(x) \quad i = 1, 2, 3, \dots, \quad (9a)$$

where

$$\Delta n_i(x) = \exp \left[ j \frac{s_i}{\pi} \int_{-\infty}^{\infty} \frac{\Delta \bar{Q}_i(\sigma)}{\sigma} \exp(-j2\pi\sigma x) d\sigma \right], \quad (9b)$$

The above equations have the advantage that the integral does not need to be recomputed when only the step size *s* is changed.

The outcome of the synthesis process depends on the *Q*-function used. We usually observed further improvements when several different *Q*-functions [Eqs. (5a–e)] were used successively for calculation of the corrections  $\Delta Q$  [Eq. (7c)]. The *Q*-functions differ considerably for low transmittances (Fig. 1), and they are highly nonlinear with *T*. The derivatives  $dQ/dT$  characterize the sensitivity of the correction process to transmittance errors. In a given problem, *T* varies with wavelength, and a good spectral fit will be achieved first in those spectral regions in which  $dQ/dT$  is largest. For example, the *Q*-function  $Q_3$  will favor the regions where *T* is low, whereas the opposite is true for  $Q_2$ . For the *Q*-function  $Q_5$  the derivative  $dQ_5/dT$  is fairly constant over a wide range of transmittances, and this results in a more uniform fit throughout the spectrum.

Clearly, the design process becomes more difficult as the transmittance *T* decreases, because the *Q*-functions are less valid. We assume in this paper that *T* has reasonable values, although we observed that in practice surprisingly low transmittances can be accommodated. How low depends on the complexity of the spectral requirements. The numerical examples described below are conservative in this respect. Further details will be given elsewhere.

## C. Determination of the Phase $\psi_i(\sigma)$ of the Corrections

The phases  $\phi_1(\sigma)$  and  $\psi_i(\sigma)$  in Eq. (7) are two other key parameters in our correction process. We now propose a method for their determination.

Following Sossi, it is possible to maintain the same

arbitrary spectral phase variation throughout the calculations [Eqs. (2), (7)]:

$$\psi_i(\sigma) = \phi_i(\sigma) \quad i = 1, 2, 3, \dots \quad (10)$$

This is valid when there is no limitation on the overall thickness. Any phase that varies smoothly with  $\sigma$  is adequate, provided that the spectral performance of the resulting refractive index profile is the only concern.

When the synthesized films are to be truncated, a suitable definition of  $\phi_1(\sigma)$  and  $\psi_i(\sigma)$  becomes essential for proper convergence of the design process. We observed that a bad choice of these two quantities could lead to very unattractive solutions. Equation (4) suggests that the following definitions might be appropriate whenever the reflectance is not too high:

$$\phi_1(\sigma) = \arg\left[\frac{r(\sigma)}{t(\sigma)}\right], \quad (11a)$$

$$\psi_i(\sigma) = \arg\left[\frac{r(\sigma)}{t(\sigma)}\right], \quad i = 1, 2, 3, \dots \quad (11b)$$

In our process, the phase  $\psi_i(\sigma)$  is calculated from Eq. (11b), where the right-hand side is the phase of the film obtained from the previous iteration or that of the starting design obtained from the main program.

Equation (11a) cannot be used directly to define  $\phi_1(\sigma)$  at the outset of the synthesis because the phase of a filter is rarely specified and especially not in this form. On the other hand, assuming that a good solution of the problem is known from previous experience, its phase  $\arg(r/t)$  can be calculated and used to define  $\phi_1(\sigma)$ . In such cases we found that a synthesis with the present method consistently yielded excellent results. This was verified several times with different transmittance targets. An example is given later. In practical situations, such phase information is usually not available since the solution is unknown initially. Numerical experiments of this kind are, therefore, in a way academic. It appears nevertheless that the definition of the phases given in Eq. (11) is correct and, in particular, that there is at least one choice for the spectral variation of  $\phi_1(\sigma)$ , which is good but usually unknown.

Even when less ideal forms of  $\phi_1(\sigma)$  were selected, we found that the definition of  $\psi_i(\sigma)$  in Eq. (11b) was still useful. Clearly, the film known at the start of each iteration in the correction process is the best film found up to that point. Accordingly its phase  $\arg(r/t)$  should be an improved  $Q$ -phase. The overall  $Q$ -phase in Eq. (7a) is thus incremented progressively in the right direction, and we noticed that it converged approximately to the phase  $\arg(r/t)$  of the synthesized film when a good solution could be found.

We also observed that such a definition of  $\psi_i(\sigma)$  resulted in more constructive corrections when the films were truncated. (In practical problems this is usually the case.) This can be explained as follows. Since Eq. (7) deals with the  $Q$ -functions, the effect of the truncation can be included explicitly into an effective  $Q$ -function  $\tilde{Q}$  defined as follows:

$$\frac{\tilde{Q}'(\sigma)}{\sigma} = 2a \int_{-\infty}^{\infty} \frac{\tilde{Q}(u)}{u} \text{sinc}[2a(\sigma - u)] du, \quad (12)$$

where  $\text{sinc}(x) = (\sin \pi x)/\pi x$ . Equation (12) is obtained by inverting the Fourier transformation in Eq. (1) after neglecting the refractive index changes for points  $|x| > a$ . The correction  $\Delta\tilde{Q}$  added to  $\tilde{Q}$  in Eq. (7) is constructive if, taking the truncation into account, the effective correction  $\Delta\tilde{Q}'$  is in phase with  $\tilde{Q}'$ . We observed that the phase  $\psi'_i(\sigma)$  of  $\tilde{Q}'$  is approximately equal to  $\arg(r/t)$ . Therefore,  $\psi_i(\sigma)$  should be such that  $\psi_i(\sigma) \approx \arg(r/t)$ . We have set  $\psi_i(\sigma) \approx \psi'_i(\sigma)$  in Eq. (11) for simplicity. This is convenient because most of the computations necessary for the evaluation of  $\psi_i(\sigma)$  have to be performed in any case to determine the spectral performance of the corresponding film. We found that the results of the synthesis deteriorated without this phase substitution.

Finally, the factorization of the phase factor  $\exp(i\psi)$  in Eq. (7b) is a simplification. It implies that the phases  $[\arg(r/t)$  and the effective  $Q$ -phase, which are similar] vary slowly from one iteration to the next. We found this to be true in general, except perhaps during the first few iterations when the errors  $\Delta Q$  are still important. The phase stabilizes itself automatically when the method starts to converge.

### C. Determination of the Initial $Q$ -Phase $\phi_1(\sigma)$

The correction process described above is fairly well behaved. In general, it yields a significant improvement over the results obtained with the standard Fourier transform method. However, the final performance still depends on the choice of the initial  $Q$ -phase  $\phi_1(\sigma)$ . This is especially true when the refractive index profiles are truncated.

Further improvements can sometimes be made if the whole synthesis is repeated with a new  $\phi_1(\sigma)$  equal to the phase of the synthesized film [Eq. (11a)]. For a new problem to which no solution is known, we specify  $\phi_1(\sigma)$  by trial and error. Simple spectral phase variations have a predictable effect on the shape of the refractive index profile and spectral performance.<sup>9,10</sup> Phase shifts can be introduced manually in selected spectral positions. This can be done rapidly and is illustrated in Sec. IV.

We have also developed a subroutine for the refinement of  $\phi_1(\sigma)$ . It is based on the observation that the errors due to the truncation can often be reduced significantly by properly configuring the starting design with the help of  $\phi_1(\sigma)$ . We assume that a reasonably good film can be synthesized by refining  $\phi_1(\sigma)$  alone. This implies that the  $Q$ -function is sufficiently accurate, that the thickness is large enough, and that the specifications include the whole spectral region where the reflectance is significant. The calculations are performed directly with the  $Q$ -function. The change in the effective  $Q$ -function  $\tilde{Q}'$  due to a phase change  $\delta\phi$  is found with Eq. (12), and the new  $Q'$  is compared with the desired  $Q$ -values  $Q(T_D)$ . We know that by definition  $Q'$  reduces to an ordinary  $Q$ -function  $Q$  when the truncation is eliminated. The process is stopped when

the errors in  $Q$  are minimized. In principle, when that occurs, the error in  $T$  is also close to a minimum.

Some of the assumptions above are not strictly valid in practice. Since the available  $Q$ -functions are accurate only for low reflectances, most of the time the desired  $Q$ -values are not known with precision, and they are not exactly equal to  $Q(T_D)$ . The errors in  $Q$  and  $T$  are probably not minimized simultaneously either. Nevertheless, we found that this phase refinement subroutine still yielded useful results.

Our subroutine uses the steepest descent refinement method. The phases

$$\phi_m = \phi(\sigma_m) \quad m = 1, 2, 3, \dots \quad (13)$$

at each wavenumber are incremented to  $\phi_m + \delta\phi$  one at a time, and the changes in  $\bar{Q}'$  are calculated. The new  $\bar{Q}'$  has a magnitude of

$$Q_m^+(\sigma) = [Q'(\sigma)]^2 + [\Delta Q'_m(\sigma)]^2 + 2Q'(\sigma)\Delta Q'_m(\sigma) \sin[\phi'(\sigma) - \phi_m]^{1/2}, \quad (14)$$

where  $\bar{Q}'$  is obtained from Eq. (12),  $\phi'$  is its phase,

$$\Delta Q'_m(\sigma) = 2\alpha\sigma \delta\phi \partial\sigma \frac{Q(\sigma_m)}{\sigma_m} \text{sinc}[2a(\sigma - \sigma_m)], \quad (15)$$

and  $\delta\sigma$  is the wavenumber increment ( $\sigma_{m+1} - \sigma_m$ ). The errors in  $Q'$  are characterized with a new merit function analogous to Eq. (8):

$$M_Q = \left( \frac{1}{N} \sum_{i=1}^N \left\{ \frac{Q'(\sigma_i) - Q[T_D(\sigma_i)]}{\delta Q(\sigma_i)} \right\}^2 \right)^{1/2}, \quad (16)$$

where the  $\delta Q$  terms are the tolerances in the  $Q$ -function. The error in the incremented function  $Q_m^+$  is calculated in a similar way and denoted by  $M_Q(\phi_m + \delta\phi)$ . This operation is repeated for each  $\sigma_m$  and the gradient of the merit function values

$$(\nabla M_Q)_m = \frac{\partial M_Q}{\partial \phi_m} = \frac{1}{\partial \phi} [M_Q(\phi_m + \partial\phi) - M_Q(\phi_m)] \quad (17)$$

is defined. Finally, the phase vector  $(\phi_1, \dots, \phi_m)$  is incremented in the direction of  $\nabla M_Q$ :

$$\phi_{m,\text{new}} = \phi_{m,\text{old}} - s(\nabla M_Q)_m, \quad (18)$$

and the step size  $s$  is optimized. This is done by calculating a new refractive index profile, the corresponding  $\bar{Q}'$  (by computing the inverse Fourier transform of the refractive index profile), and the value of its merit function.

Speed is the main advantage of working directly with the  $Q$ -functions in this refinement method. A more accurate but much slower alternative would be to calculate a refractive index profile and its spectral performance for each new phase. For the reasons stated above our implementation is approximate, but nevertheless we found that it yielded initial  $Q$ -phases with which better starting designs could be synthesized.

## IV. Numerical Tests

### A. General Remarks

In Fig. 3 (and subsequent similar figures), the two diagrams in the same row represent one set of results. In the left diagrams, the desired transmittance and initial  $Q$ -phases are represented by heavy lines. Thinner lines are used to depict the calculated transmittances and phases  $\arg(r/t)$ . When two calculated transmittance curves are shown, curves 1 and 2 correspond to the performance of the system before and after using the correction process. In the diagrams on the right, the synthesized refractive index profiles are plotted against the optical thickness measured from the center outward. The refractive indices of the surrounding media have both an average value equal to  $1.78 = (1.35 \times 2.35)^{1/2}$ . The values of the main parameters used in the synthesis are listed in Table I.

Speed is important for an iterative process where refractive index profiles and their spectral performance have to be computed a number of times. To represent a graded index film accurately it is necessary to sample the refractive index variations at a large number of points. In this work, we use approximately six points per quarterwave optical thickness at the central wavenumber (i.e., an average of twelve points between two successive maxima of the refractive index profiles). The points are separated by equal optical thickness increments. Each pair of points delimits a sublayer which is considered to have a linear variation of the refractive index. The characteristic matrices of such layers are known<sup>14</sup> and could be used to compute the spectral curves. However, we found that the computations were faster and still yielded good results when the gradual variation of the refractive indices was replaced with an average value:

$$\bar{n} = 1/2(n_a + n_b), \quad (19)$$

where  $n_a$  and  $n_b$  are the refractive indices at the interfaces of the layer. This means that a graded index film is eventually approximated with very thin homogeneous layers with identical optical thicknesses. In spite of the large number of matrix multiplications, the computation of the spectral performance is fast because the sine and cosine of the common phase thickness need to be computed only once for each wavelength at the outset of the calculation.

By contrast, our discretization subroutine selects the refractive indices and the boundaries of the homogeneous layers so that the graded index film is approximated as closely as possible. In general this results in unequal optical thicknesses, and the calculations are slower.

The values of the merit function (here with uniform tolerances of 1% unless otherwise stated) and the CPU time are recorded in each iteration of our correction process. The times cited in our examples refer to the synthesis *per se*, and they are indicative of a typical run. Neither the program nor the choice of parameters and options used in the numerical examples has been fully optimized for speed. The present version of

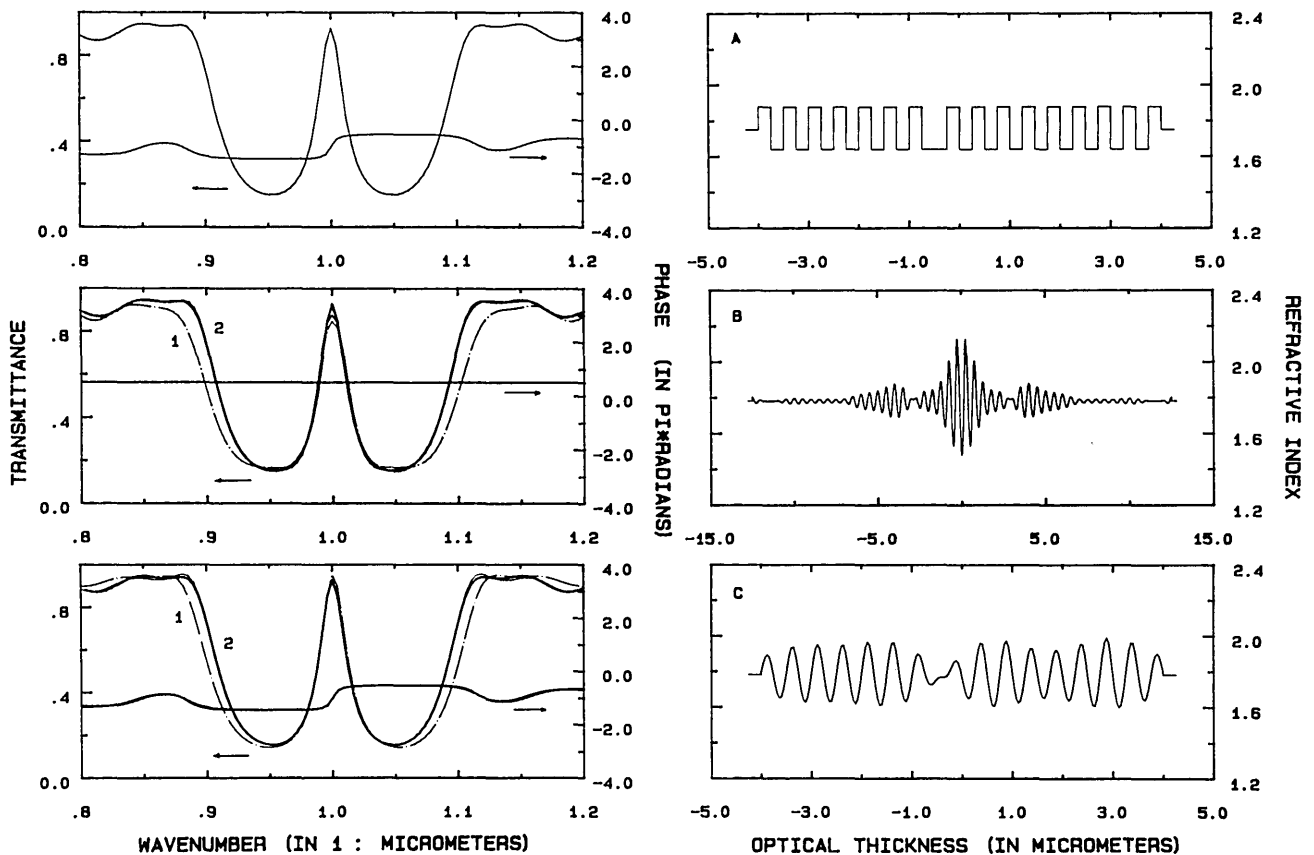


Fig. 3. Synthesis examples showing the importance of the initial  $Q$ -phase.

the program does not use fast Fourier transforms. The calculations were performed on a HP 1000 model A700 microcomputer.

#### B. Ideal Cases

As an example, a synthesis exercise is performed where the target is the transmittance of the multilayer system represented in Fig. 3(A). The multilayer is, therefore, an exact solution. It is a slightly asymmetrical bandpass interference filter composed of quarter-wave and halfwave layers. We have chosen a simple system for tutorial purposes. Nevertheless the reflectance is significant ( $\sim 80\%$ ), and the passband is relatively sharp. In addition, the solution will be a graded index film, whereas the multilayer is homogeneous. These points constitute an interesting test for the correction method. The question arises: Is it possible to retrieve a good solution comparable to the multilayer and if so in what conditions? The important role of the initial  $Q$ -phase  $\phi_1(\sigma)$  is discussed in this connection.

In Fig. 3(B), the optical thickness is large and  $\phi_1(\sigma)$  is assumed to be constant. The spectral fit obtained directly without using the correction subroutine is already quite good (curve 1), and the computation took only a few CPU seconds. The transmittance obtained after corrections can barely be distinguished from the target (curve 2). The phase  $\arg(r/t)$  remained equal to the initial  $Q$ -phase in spite of the phase substitutions

[Eqs. (7b) and (11)]. The synthesized film has a pronounced bell shape, which is typically associated with a constant phase.<sup>10</sup> It differs markedly from the initial multilayer. About 190 s were required for the whole synthesis.

The above example illustrates that the choice of  $\phi_1(\sigma)$  is simple when no limits are imposed on the optical thickness. We found that any phase with a smooth spectral variation is acceptable, at least as far as the spectral fit is concerned. This is no longer true when the thickness is limited. We could not find a good solution to the above problem when the optical thickness was reduced to that of the multilayer. However, we obtained a very good result when  $\phi_1(\sigma)$  was set equal to the phase  $\arg(r/t)$  of the multilayer [Fig. 3(C)]. In spite of the smaller thickness several observations made in connection with the previous diagram are still true. The fit of both transmittance curves (1 and 2) did not deteriorate, and the final phase  $\arg(r/t)$  remained essentially equal to the initial  $Q$ -phase  $\phi_1(\sigma)$ . Furthermore, the synthesized film is more similar to the original multilayer. The halfwave layer near the center is clearly apparent and surrounded by two nearly periodic film sections. The index variations are now gradual because the transmittance of the initial multilayer has higher harmonics, which were not included in the target transmittance. There are no higher harmonics in the transmittance of the synthesized film. Finally the computations were very fast. Curve 1 in

Table I. Parameters Used in the Numerical Examples

Figure: curve	Optical thickness ( $\mu\text{m}$ )	Q-functions	$\phi_1(\sigma)^1$	Options <sup>2</sup>	Remarks <sup>3</sup>
3(B)	25	$Q_5$	$C$	$W, C_1$	
3(C)	8	$Q_5$	$M$	$W, C_1$	
5(A)	8	$Q_5$	$G$	$W, C_1$	
5(B)	8	$Q_5$	$S$	$W, C_1$	
5(C)	8	$Q_5$	$G$	$W, C_1$	$a$
5(D)	8	$Q_5$	$G$	$W, PR$	
5(E)	8	$Q_5$	$S$	$W$	$b$
6(A)	4	—	—	$REF$	$c, d$
6(B)	4	$Q_5$	$T$	$W, C_1$	$c$
6(C)	4	$Q_3$	—	$C_2$	$c, d$
6(D)	4	$Q_5$	$T$	$W, C_1$	$c, e$
		$Q_3$	—	$C_2$	$c, d, e$

<sup>1</sup> Several different initial Q-phases  $\phi_1(\sigma)$  are used:  $C$ , constant ( $\pi/2$ );  $M$ , calculated phase  $\arg(r/t)$  of the multilayer [Fig. 3(A)];  $G$ , Gaussian (centered at  $\sigma = 1 \mu\text{m}$ , halfwidth =  $0.2 \mu\text{m}$ , height =  $\pi$  rad);  $S$ , phase  $\arg(r/t)$  of the film synthesized previously;  $T$ , proportional to the desired transmittance  $T_D(\sigma)$  with a maximum phase variation of  $1.5\pi$  rad.

<sup>2</sup> Options used in the synthesis:  $W$ , Fourier transform method without corrections;  $C_1$ , fast version of the correction process;  $C_2$ , alternate version of the correction process with complete optimization of the step size;  $PR$ , refinement of the phase  $\phi_1(\sigma)$ ;  $REF$ , refinement of the layer thicknesses and indices.

<sup>3</sup> Remarks:  $a$ ,  $\phi_1(\sigma)$  has a phase jump of  $\pi$  rad at  $\sigma = 1 \mu\text{m}$ ;  $b$ ,  $\phi_1(\sigma)$  is flipped upside down for wavenumbers larger than  $1.13 \mu\text{m}^{-1}$ ;  $c$ , the minimum acceptable convergence rate for the values of the merit function is set to 1% instead of 5% by default;  $d$ , the tolerances are set to 0.1% at the wavelengths where  $T$  is minimum ( $\lambda \approx 0.55 \mu\text{m}$ ) instead of 1% by default;  $e$ , the graded index film is discretized.

Fig. 4 shows that the values of the merit function were reduced to below 1 in  $\sim 30$  s. At that point the average error in transmittance was within the 1% tolerance. These results will be used for comparison purposes in the following.

We repeated this experiment a number of times with other more complex targets, and we consistently obtained good results. This confirms the suggestion that the phase  $\arg(r/t)$  of the original multilayer is an excellent initial Q-phase. Note that the Q-function used in the above examples was not  $\bar{Q} = r/t$ . Its magnitude was  $|Q_5|$  instead of  $|Q_3|$  [see Table I and Eq. (5)]. We found that this combination often gave better results, especially for higher reflectances.

### C. Simulation of an Unknown Q-Phase

In practice, the appropriate spectral variation of  $\phi_1(\sigma)$  is unknown at the outset of the synthesis process. To simulate such a situation, we repeated the previous synthesis with a different form of  $\phi_1(\sigma)$ . A Gaussian phase shape was chosen in Fig. 5(A), because this is known to result in a more uniform refractive index profile.<sup>10</sup> Here the Gaussian had approximately the same halfwidth and the same center of gravity as the desired transmittance. Its height was quickly adjusted by trial and error until the shape of the refractive index profile appeared to be acceptable.

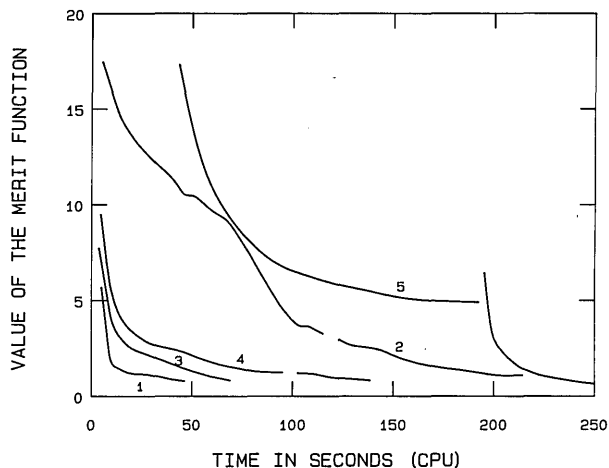


Fig. 4. Variation of the value of the merit function with time for Figs. 3(C) and 5(A)–(D) (see text).

The spectral fit obtained in this example before calling the correction process is quite poor (curve 1). The passband is completely ignored. Nevertheless, the transmittance obtained with the correction subroutine nearly coincides with the target (curve 2).

The behavior of the phases is interesting. The physical phase of the synthesized film is now significantly different from the initial Gaussian Q-phase. It exhibits shifts of  $\pi$  rad at the wavenumbers corresponding to the transmittance maxima. The deeper and narrower the passbands, the sharper the shifts. A similar behavior is observed for the phase of the original multilayer, although the shifts do not occur in the same directions [for example, the phase at  $\sigma = 1 \mu\text{m}^{-1}$  decreases in Fig. 5(A), whereas it increases in Fig. 3(A)].

The synthesized refractive index profile has little in common with the multilayer. The large refractive index change at the right end is characteristic and indicates that a larger thickness would have been useful. This is not unexpected. In each iteration, the program calculates only the central portion of the refractive index profile, up to the maximum thickness specified. The rest is ignored. The detrimental effect of this truncation depends on the choice of the initial Q-phase.

The convergence of the computations in this example is somewhat slower and more laborious than before, although it is still quite creditable—the whole synthesis took  $\sim 210$  s (Fig. 4, curve 2). The small glitches in this curve indicate that the step size was (automatically) readjusted several times in the course of the correction process. The gap means that the process stalled and was restarted manually with a new Q-function (Table I).

The film synthesized here does not seem very attractive, but it has a good spectral performance. There are cases in which it is not even possible to obtain a good spectral fit. When this happens other forms of the initial Q-phase  $\phi_1(\sigma)$  can be tried. For example, one can (1) change the amplitude and halfwidth of the

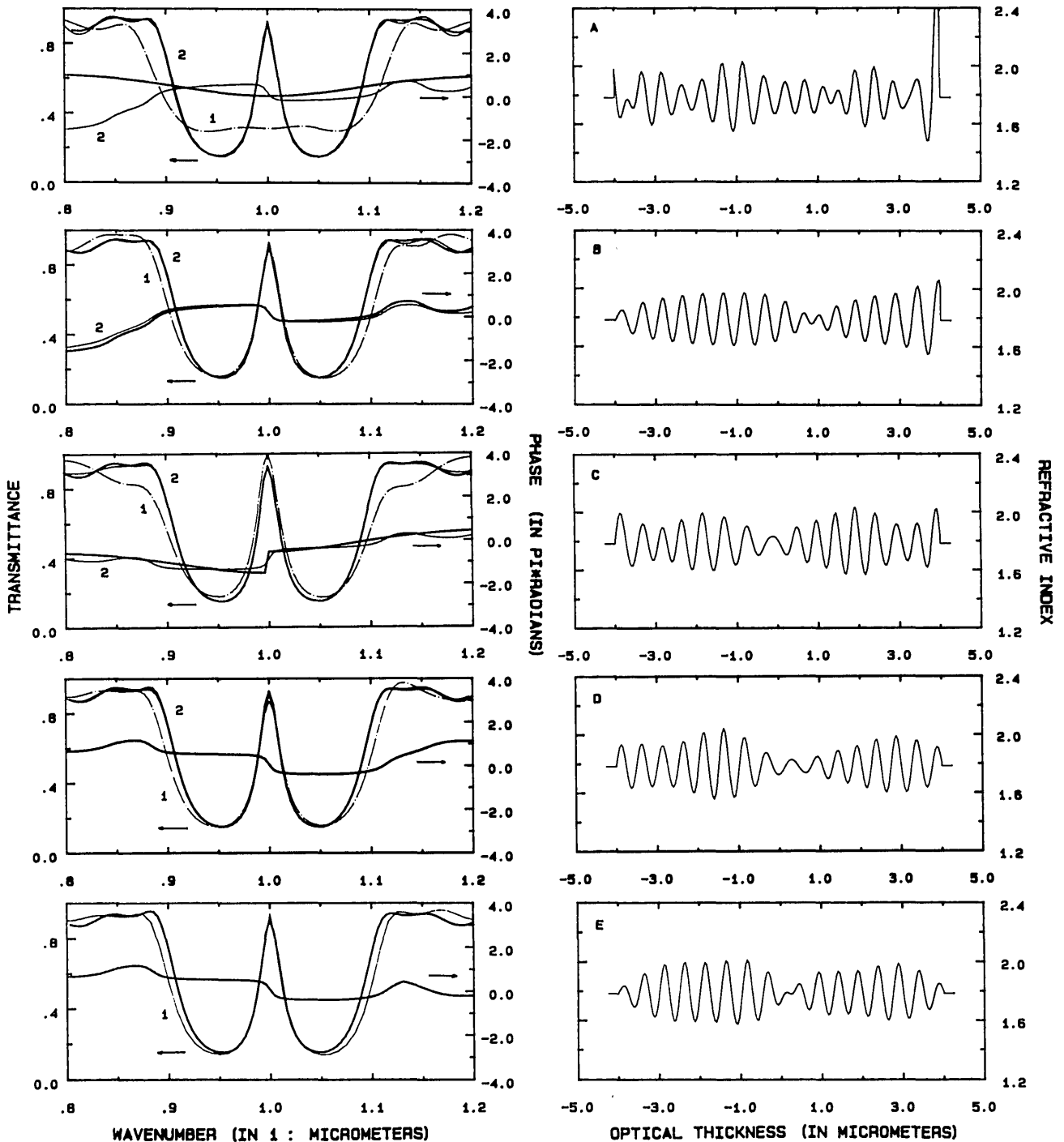


Fig. 5. Synthesis examples with full determination of the  $Q$ -phase.

Gaussian, (2) use a completely different phase shape, for example, proportional to the transmittance curve, (3) set  $\phi_1(\sigma)$  equal to the calculated phase  $\arg(r/t)$  of the synthesized film, since the latter is in general better than the starting design, (4) introduce phase shifts manually at input, (5) refine  $\phi_1(\sigma)$ . The last four options are illustrated in the following. We found often that the phase refinement was more reliable but slower than the other options.

#### D. Optimization of the Phase

In Fig. 5(B), the synthesis was repeated with a new  $\phi_1(\sigma)$  set equal to the phase  $\arg(r/t)$  calculated in the preceding diagram. The spectral fit obtained after corrections is not improved (this is not necessary), but the refractive index profile is much smoother than before. It is still quite different, however, from the original multilayer. The calculated phase is similar to

$\phi_1(\sigma)$ , except that it has been slightly tilted. The calculations were fast (70 s, see Fig. 4, curve 3). However, the total time for this synthesis must include the 210 s already spent to obtain  $\phi_1(\sigma)$ . The quality of the final result is quite comparable with that illustrated in Fig. 3(C).

In Fig. 5(C), a phase jump of  $\pi$  rad was superimposed manually to the Gaussian  $\phi_1(\sigma)$  at the wavenumber corresponding to the transmittance peak. As a result a deep passband was created from the start (curve 1). Again, the spectral fit obtained after corrections is excellent (curve 2). The synthesized refractive index profile is relatively smooth, and additional phase shifts have been created by the correction process. The profile and phase shifts are different from those illustrated before. The calculations were relatively fast (140 s; see Fig. 4, curve 4), but they were again appreciably slower than those for our reference case [see Fig. 3(C) and Fig. 4, curve 1].

In Fig. 5(D), the initial Gaussian  $Q$ -phase  $\phi_1(\sigma)$  was refined before the correction subroutine was called. The transmittance curve 1 was obtained after the phase refinement but before the corrections. Curve 2 was found after the corrections. Remarks similar to those made in the previous examples concerning the spectral fit, phase shifts, and refractive index profiles are also valid here.

The phase refinement is responsible for a large part of the computation time. Yet the total time required for the synthesis remains reasonable. It is of the order of 250 s (Fig. 4, curve 5). The first section of curve 5 pertains to the phase refinement and the second section to the correction process *per se*. The values of the merit function are discontinuous at the junction because two different merit functions were used. Note the very fast convergence in the second section. This means that the phase  $\phi_1(\sigma)$  produced by the phase refinement is excellent.

We have found so far four different films which offer a very good spectral performance [Figs. 3(C), 5(B)–(D)]. The corresponding phases are different, although they have several common features. There are phase shifts at the wavenumbers corresponding to the transmittance maxima. At the transmittance minima, the phases have either an inflection point or a zero derivative. The phase variation is similar between two successive transmittance minima, except that it may be flipped upside down. This can be exploited to control the shape of the refractive index profile.

To illustrate this point, the synthesis was repeated with a new  $\phi_1(\sigma)$  set equal to the physical phase calculated in the preceding example but flipped upside down for wavenumbers larger than  $1.13 \mu\text{m}$ . The resulting  $\phi_1(\sigma)$  and the refractive index profile synthesized directly without the help of any correction or phase refinement are illustrated in Fig. 5(E). The spectral performance is already quite good and comparable with that obtained in similar circumstances in Fig. 3(C) (curve 1). This means that the phase flip did not cause a significant deterioration of the  $Q$ -phase. After corrections, the spectral fit became excellent.

Because the refractive index profile and the phase changed only slightly, they were not plotted for the sake of clarity. The refractive index profile shown here bears a strong resemblance to that illustrated in Fig. 3(C), although there are still some differences. The profiles and phase curves would become even more similar if the phase  $\phi_1(\sigma)$  in Fig. 5(E) were flipped again for wavenumbers larger than  $0.95 \mu\text{m}$ .

It is usually not easy to predict the effect of a phase flip on the refractive index profile. Unless insight is gained from previous experience, it might be useful to try all possible flip combinations. In this example, there are four positions where the phase can be flipped up or down, namely, at  $0.87$ ,  $0.95$ ,  $1.05$ , and  $1.13 \mu\text{m}$ . Five different combinations have been illustrated in Figs. 3(C) and 5(B)–(E).

#### E. Additional Remarks

The numerical exercise described above was performed a number of times with different targets. A superior result was always obtained when the initial  $Q$ -phase  $\phi_1(\sigma)$  was equal to the phase  $\arg(r/t)$  of the multilayer. The synthesized film was with rare exceptions a graded index version of the multilayer. This might be viewed as a practical method of transforming a homogeneous system into a graded index film.

Our results show that several different designs with a performance that is as good as that of the multilayer can be found when other forms of  $\phi_1(\sigma)$  are used. The computations are extremely fast when a suitable  $\phi_1(\sigma)$  can be found. A large fraction of the CPU time is often spent in the determination of  $\phi_1(\sigma)$ .

#### V. Comparison with Other Methods

Contrary to the assumption made in the preceding section, a typical problem in thin film design rarely has an exact solution. Nevertheless, the spectral performance which is obtained should be in reasonable agreement with the specifications. We describe below a synthesis exercise performed with a completely arbitrary target (Fig. 6). The latter is the outline of a monument illustrated in the logo of the Seventh International Conference on Thin Films. This target has been used previously for the intercomparison of different design methods.<sup>13</sup> The correction process is now tested against these published results.

First, the optical thickness of the film must be estimated and kept as small as possible. It must, however, be sufficient to allow for a good spectral fit in the most critical wavelength region, namely, here in the narrow stopband located at  $\lambda = 0.55 \mu\text{m}$ . The minus filter theory predicts that a minimum of  $\sim 6 \mu\text{m}$  optical thickness is required.<sup>13,15</sup> This is also adequate here for obtaining a proper performance over the entire spectral range. We have nevertheless chosen to reduce the optical thickness to  $4 \mu\text{m}$  in Fig. 6 for direct comparison with several interesting examples of Ref. 13. The spectral fit is not quite as good as when the

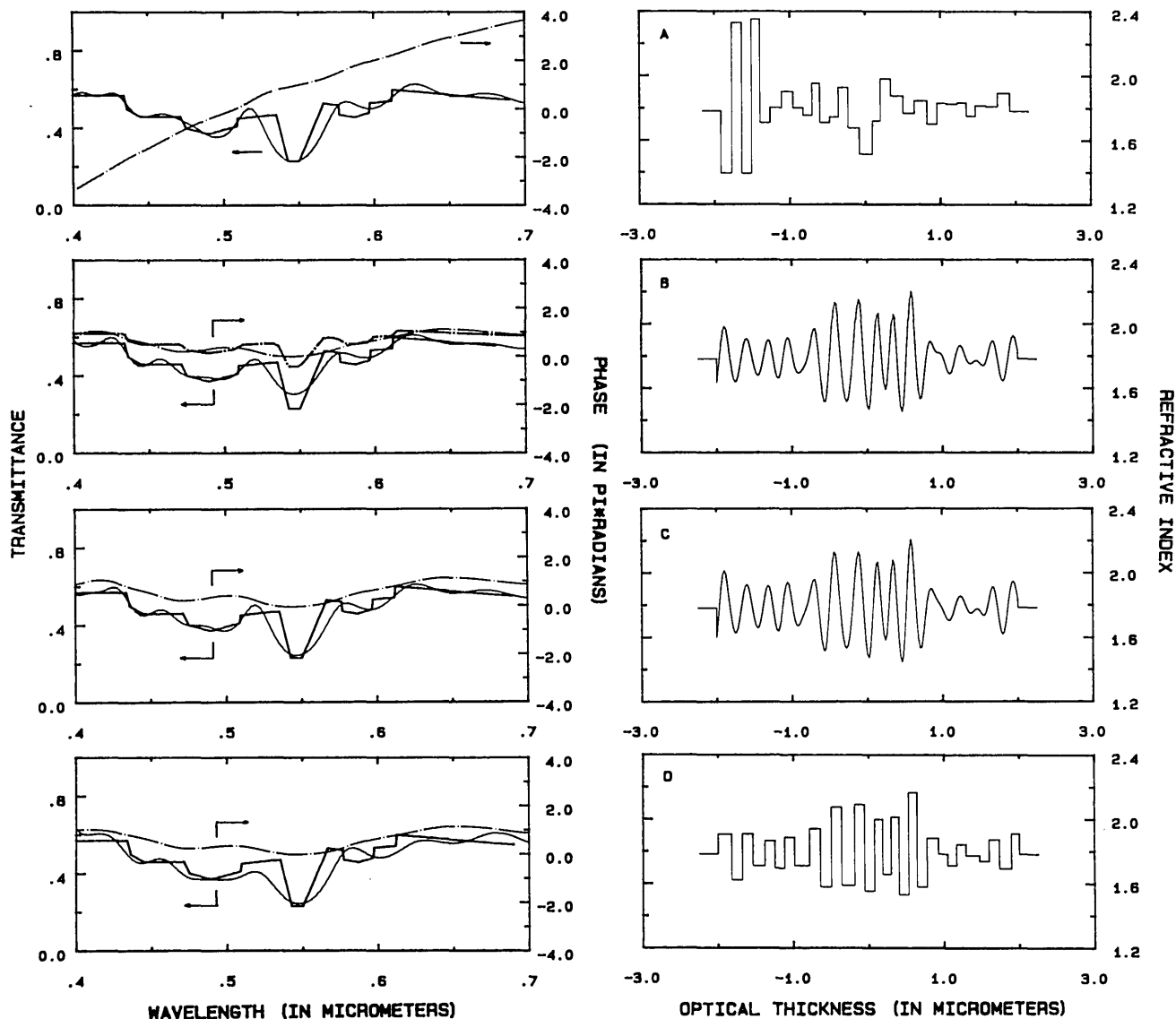


Fig. 6. Comparison of the correction process with refinement.

estimated thickness is used, but the results show that a useful approximate solution can be found with the correction process.

All the methods discussed in Ref. 13 involved a refinement stage in the end. They yielded homogeneous multilayer systems, which, although they were quite different, had a comparable spectral performance for a given overall thickness. Presumably this means that the accuracy which was achieved was nearly optimum in the circumstances. Figure 6(A) illustrates a typical result found by refinement alone after a suitable starting design was identified. This diagram is similar to Fig. 3 of Ref. 12. (The calculated multilayers are different, however. For consistency with the preceding sections, the refractive indices were forced here to have values between 1.35 and 2.35. The refractive index of the external media and the mean refractive index in the starting design were raised to 1.78. This has no effect on the spectral fit.)

The time spent for refinement in this example was of the order of 790 s. Part of the variation of the value of the merit function  $M$  against time is illustrated in Fig. 7, curve 1. The final value of  $M$  was 4.6. Both the layer thicknesses and refractive indices were adjusted. We used an old but effective routine similar to the Golden Section method. Additional details can be found in Table I.

Figure 6(B) shows a result computed with our correction process. The initial  $Q$ -phase  $\phi_1(\sigma)$  was proportional to the desired transmittance with a maximum excursion of  $1.5\pi$  rad. No refinement was involved, and the computation was extremely fast (55 s; see Fig. 7, curve 2a). Nevertheless the overall spectral performance of the synthesized graded index film compares advantageously with that of the homogeneous multilayer illustrated in the preceding diagram. The maximum reflectance in the stopband at  $\lambda = 0.55 \mu\text{m}$  is not large enough, but the halfwidth is better than before.

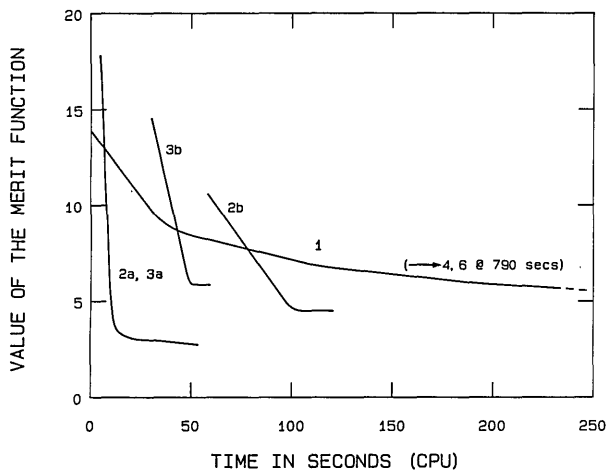


Fig. 7. Variation of the values of the merit function with time for Figs. 6(A)–(D) (see text).

It is possible to gain some reflectance in the stopband at the expense of the halfwidth. To obtain Fig. 6(C), the correction process was restarted with three modifications. First, tighter tolerances were imposed around  $\lambda = 0.55 \mu\text{m}$  [0.1% instead of 1%; these same values were used in the calculations for Fig. 6(A)]. Second, the  $Q$ -function was changed from  $Q_5$  to  $Q_3$  to increase the sensitivity  $dQ/dT$  to the transmittance errors for low values of the transmittance. Third, we used the alternate version of the correction process in which the step size is fully optimized during each iteration. This version is more sensitive to the modulation of the tolerances. The additional time for the computation was  $\sim 65$  s for a total of  $\sim 120$  s (Fig. 7, curves 2a, 2b). This is much faster than the 790 s required to obtain the results of Fig. 6(A), yet the quality of the spectral fit is the same.

The time savings would be even more important had the comparison been made with the time required to design a graded index film by refinement. The refractive index profile would then have to be subdivided in a very large number of thin layers, and the computation time could then easily be multiplied by a factor of 5 or 10. Special care would also probably be needed to ensure that the refractive index profile obtained by refinement is gradual.

Finally, the correction process can also be used to design a homogeneous multilayer system. To obtain Fig. 6(D), the sequence of operations performed in the previous example was repeated, except that the graded index film calculated during each iteration was discretized. Once again the calculations were very fast ( $\sim 60$  s, see Fig. 7, curve 3b; for times  $< 30$  s, the values of the merit function closely follow curve 2a). The spectral performance of the synthesized multilayer is not quite as good as that of the graded index film depicted in Fig. 6(C). This is not very surprising because the discretizations performed here were rather crude. The number of layers was kept the same as in Fig. 6(A). The spectral fit would have been better had the graded index films been approximated more closely with many more thin layers. We observed a significant

improvement with forty layers (instead of twenty-nine), and the computations did not take much longer. Alternatively, it could be possible to refine the multilayer illustrated in Fig. 6(D). We found that this refinement was not much faster than the one performed to obtain Fig. 6(A) (450 vs 790 s). This is not surprising because the starting designs were quite good in both cases. However, with the Fourier transform method the starting design is obtained rapidly and conveniently.

Some remarks about the phases in the above examples are interesting. The phase  $\arg(r/t)$  represented in Fig. 6(A) is almost linear. We know that when this phase is constant, large refractive index changes occur near the center of the refractive profile [see Fig. 3(B), for example]. Here the phase is tilted, and the large refractive index changes are observed near one end of the profile. This is consistent with previous knowledge.<sup>9,10</sup> Finally, we found no improvement in Figs. 6(B)–(D) when the initial  $Q$ -phase  $\phi_1(\sigma)$  was refined. This is probably because no sharp phase shifts were required.

## VI. Conclusion

A key element in the Fourier transform method is a complex spectral function  $\tilde{Q}(\sigma)$  through which the desired transmittance is accounted for. Exact explicit expressions for the magnitude and phase of this function are yet to be found. In this paper, we describe an iterative numerical process where successive corrections are made to  $\tilde{Q}(\sigma)$ . This procedure compensates automatically for the imprecision in the available definitions of  $\tilde{Q}(\sigma)$  and for several other types of error. These include errors which occur when the refractive index variations are neglected beyond a certain maximum overall thickness (truncation), when the refractive indices are forced to lie between maximum and minimum values ( $n_H, n_L$ ), or when the graded index films are approximated by homogeneous multilayers. The accuracy and versatility of the Fourier transform method are thus significantly improved.

The performance of the correction process has been illustrated and tested with a number of numerical examples. Several practical issues have been demonstrated. In particular, it is shown that the thickness of the synthesized films can be reduced significantly if the complex phase of  $\tilde{Q}(\sigma)$  is defined appropriately. This phase can also be used to modify the shape of the refractive index profile without affecting the spectral performance. This is done by flipping the phase curve upside down in certain parts of the spectral range. A simple method of transforming a homogeneous multilayer system into a graded index film of similar performance has also been described. Finally a standard problem that was used in the past to compare different numerical design methods was solved with the present process. The latter was found to be very fast, and the quality of the results was quite comparable for a given overall optical thickness.

The authors wish to express their thanks to their colleagues F. C. Ho and B. T. Sullivan for their helpful comments.

## References

1. R. Jacobsson, "Light Reflection from Films of Continuously Varying Refractive Index," in *Progress in Optics*, Vol. 5 (North-Holland, Amsterdam, 1966).
  2. R. W. Bertram, M. F. Ouellette, and P. Y. Tse, "New Approach to Design and Production of Inhomogeneous Optical Coatings," in *Technical Digest, Topical Meeting on Optical Interference Coatings* (Optical Society of America, Washington, DC, 1988), pp. 150-153.
  3. W. H. Southwell, "Gradient-Index Antireflection Coatings," *Opt. Lett.* **8**, 584-586 (1983).
  4. W. E. Johnson and R. L. Crane, "An Overview of Rugate Filter Technology," in *Technical Digest, Topical Meeting on Optical Interference Coatings* (Optical Society of America, Washington, DC, 1988), pp. 118-121.
  5. M. Zukic and K. H. Guenther, "Optical Coatings with Graded Index Layers for High Power Laser Applications," *Proc. Soc. Photo-Opt. Instrum. Eng.* **895**, 271-277 (1988).
  6. L. Sossi, "A Method for the Synthesis of Multilayer Interference Coatings," *Eesti NSV Tead. Akad. Toim. Fuus. Mat.* **23**, 229-237 (1974) (Translation Services of the Canada Institute for Technical and Scientific Information, National Research Council of Canada, Ottawa, Ontario, Canada K1A 0R6).
  7. L. Sossi, "On the Synthesis of Interference Coatings," *Eesti NSV Tead. Akad. Toim. Fuus. Mat.* **26**, 28-36 (1977) (see Ref. 6 for translation).
  8. E. Delano, "Fourier Synthesis of Multilayer Filters," *J. Opt. Soc. Am.* **57**, 1529-1533 (1967).
  9. J. A. Dobrowolski and D. G. Lowe, "Optical Thin Film Synthesis Program Based on the Use of Fourier Transforms," *Appl. Opt.* **17**, 3039-3050 (1978).
  10. P. G. Verly, J. A. Dobrowolski, W. J. Wild, and R. L. Burton, "Synthesis of High Rejection Filters with the Fourier Transform Method," *Appl. Opt.* **28**, 2864-2875 (1989).
  11. B. G. Bovard, "Derivation of a Matrix Describing a Rugate Dielectric Thin Film," *Appl. Opt.* **27**, 1998-1905 (1988).
  12. B. G. Bovard, "Fourier Transform Technique Applied to Quarterwave Optical Coatings," *Appl. Opt.* **27**, 3062-3063 (1988).
  13. J. A. Dobrowolski, "Computer Design of Optical Coatings," *Thin Solid Films* **163**, 97-110 (1988).
  14. R. F. Potter, "Optical Properties of Lamelliform Materials," *Proc. Soc. Photo-Opt. Instrum. Eng.* **276**, 204-213 (1981).
  15. J. A. Dobrowolski, "Subtractive Method of Optical Thin-Film Interference Filter Design," *Appl. Opt.* **12**, 1885-1893 (1973).
-